

Black Carbon and the Regional Climate of California

Report to the
California Air Resources Board
Contract 08-323

Prepared by:
V. Ramanathan
Principal Investigator

| | | |
|--------------------------------|----------------------------------|-------------------------------|
| Dr. R. Bahadur ¹ | Dr. K. A. Prather ² | Dr. O. L. Hadley ³ |
| Dr. V. Ramanathan ¹ | Dr. A. Cazorla ² | Dr. R. Leung ⁴ |
| Dr. P. S. Praveen ¹ | Dr. T. Kirchstetter ³ | Dr. C. Zhao ⁴ |

¹Scripps Institution of Oceanography
University of California at San Diego

²Department of Chemistry and Biochemistry
University of California at San Diego

³Lawrence Berkeley National Lab.

⁴Pacific Northwest National Lab.

January 22 2013

DISCLAIMER

This report was prepared by the University of California, San Diego (Contractor), in association with Lawrence Berkeley National Laboratories and Pacific Northwest National Laboratories (Sub-Contractors) as an account of work sponsored by the California Air Resources Board (CARB), under contract # 08-323. The statements and conclusions in this report are those of the contractor, and not necessarily of CARB. The mention of any commercial products, their use in conjunction with material reported here, or their source is not to be construed as an actual or implied endorsement of such products.

ACKNOWLEDGEMENTS

We thank Dr. Nehzat Motallebi for project management, support, and guidance over the duration of this contract.

We thank Dr. D. Chand, Dr. B. Schmid, and Dr. H. H. Jonsson for providing measurements collected during the CalNex and CalWater field campaigns used to validate aerosol sources.

We gratefully acknowledge Dr. Ron Cohen (UC Berkeley), Dr. Surabi Menon (LBL), and Dr. Yan Feng (Argonne National Labs.) for their scientific input and additional guidance for the project.

We would also like to thank Dr. Lynn M. Russell (UCSD) for heading the associated CARB funded work constraining the indirect effect of black carbon on clouds in California.

We acknowledge the National Energy Research Scientific Computing Center (NERSC), which is supported by the U.S. Department of Energy Office of Science under Contract No. DE-AC02-05CH11231, and the PNNL Institutional Computing, for providing computing resources for the regional model simulations performed by PNNL

We would like to acknowledge the hard work and contribution of several graduate students and post graduate researchers including Yangyang Xu (UCSD), Liliana Nunez (UCSD), and Dev Milstein (LBL) who contributed in part to this work.

The work described in this report was primarily accomplished by post-graduate researchers Dr. Ranjit Bahadur (UCSD), Dr. P. S. Praveen (UCSD), Dr. Alberto Cazorla (UCSD), Dr. Odelle Hadley (LBL), Dr. Chun Zhao (PNNL), and Project PIs Prof. V. Ramanathan (UCSD), Prof. K. Prather (UCSD), Prof. T. Kirchstetter (LBL), and Dr. R. Leung (PNNL).

TABLE OF CONTENTS

List of Tables

List of Figures

List of Acronyms

Abstract

Executive Summary

- 1.0 Introduction
 - 1.1 Motivation
 - 1.2 Prior Work
 - 1.3 Research Objectives
 - 1.4 Structure of Report
- 2.0 Coefficient of Haze as a Black Carbon Proxy
 - 2.1 Introduction
 - 2.2 Operational principles
 - 2.3 Restoration and Laboratory evaluation of COH instruments
 - 2.4 Collocated measurements of BC and COH
 - 2.5 Relationship between COH and BC
 - 2.6 Conclusions
- 3.0 Historical Trends in BC concentration in California
 - 3.1 Introduction
 - 3.2 Data Sources
 - 3.3 Black carbon trends
 - 3.4 Seasonal patterns in BC
 - 3.5 Weekly patterns in BC
 - 3.6 Energy consumption trends
 - 3.7 Conclusions
- 4.0 Change in Surface BC concentration 1980-2000
 - 4.1 Introduction
 - 4.2 BC Aerosol and Diesel Emissions
 - 4.3 Temporal trends in BC Concentrations
 - 4.4 Spatial trends in BC Concentration
 - 4.5 Changes in Aerosol radiative properties
 - 4.6 Implications for direct radiative forcing
 - 4.7 Impact of Diesel Emissions Control Policies
 - 4.8 Role of urban sites and South Lake Tahoe
 - 4.9 Conclusions

- 5.0 Solar absorption by Black Carbon (BC) and Brown Carbon (BrC)
 - 5.1 Introduction
 - 5.2 Partitioning AOD
 - 5.3 Aerosol Robotic Network (AERONET)
 - 5.4 Constraining the AAE and SAE
 - 5.5 Single Scattering Albedo
 - 5.6 Concentration Independence of Intrinsic Properties
 - 5.7 Brown Carbon Absorption in California
 - 5.8 Sensitivity to AAE
 - 5.9 Estimation of Error
 - 5.10 Conclusions

- 6.0 Sources of BC and BrC aerosol particles
 - 6.1 Introduction
 - 6.2 Spectral Properties and Composition
 - 6.3 In-situ Aircraft measurements
 - 6.4 Aerosol Time of Flight Mass Spectrometry
 - 6.5 Comparison of ATOFMS and spectral classification
 - 6.6 The California case study
 - 6.7 Conclusions

- 7.0 Woodsmoke as a source of absorbing BrC
 - 7.1 Introduction
 - 7.2 Field Measurements
 - 7.3 Contribution of BC to absorption
 - 7.4 Sources of Error
 - 7.5 Results from Field Study
 - 7.6 Significance of Results
 - 7.7 Conclusions

- 8.0 Direct radiative Forcing of carbonaceous aerosols
 - 8.1 Introduction
 - 8.2 Observation of aerosol properties
 - 8.3 Partitioning of aerosol absorption
 - 8.4 Comparison with models
 - 8.5 Aerosol vertical profiles
 - 8.6 The MACR model
 - 8.7 Radiative forcing results
 - 8.8 BC reduction Scenario
 - 8.9 Conclusions

- 9.0 Surface solar flux in California
 - 9.1 Introduction
 - 9.2 The CIMIS network
 - 9.3 Variability in the CIMIS measurements

- 9.4 Filtering the clear-sky signal
- 9.5 Climatology of clear-sky flux
- 9.6 Conclusions

- 10.0 Implications to Global Warming Mitigation

- 11.0 Current emission inventories for BC
 - 11.1 Introduction
 - 11.2 Emission Scenarios
 - 11.3 The CALNEX study
 - 11.4 Conclusions

- 12.0 Radiative forcing from Regional Models
 - 12.1 Introduction
 - 12.2 WRF_PNNL model description
 - 12.3 WRF_PNNL model evaluation
 - 12.4 Estimates of radiative forcing
 - 12.5 Significance of WRF_PNNL simulations
 - 12.6 The WRF_LBL study
 - 12.7 Comparing WRF_LBL with observations
 - 12.8 Radiative forcing from WRF_LBL
 - 12.9 Conclusions

- 13.0 Regional climate impacts of BC
 - 13.1 Introduction
 - 13.2 Numerical Experiments
 - 13.3 WRF_PNNL: Effects of BC on California climate
 - 13.4 WRF_LBL: Effects of BC on California climate
 - 13.5 Conclusions

- 14.0 Conclusions
 - 14.1 Primary Conclusions
 - 14.2 Research Highlights

- References

LIST OF TABLES

Table 4.1 Annual mean and standard deviations of measured Black Carbon concentration and BC/non-BC Aerosol ratios in California. Rates of change are calculated based on a linear fit for annual mean values between 1989 and 2008.

Table 5.1 AERONET sites used to obtain AOD and AAOD measurements.

Table 5.2 Absorption Angstrom exponents for dust, total carbon, BC, and OC determined in this study and the ranges reported in the literature.

Table 5.3 Wavelength dependent Single Scattering Albedo determined in this work compared with literature values.

Table 5.4 Dust, OC, and BC fraction of the total AAOD and AOD as determined from AERONET (this work) and the GOCART model in California

Table 5.5 Sensitivity of AAOD partitioning to choice of AAE for the California case study.

Table 6.1 List of the AERONET stations around the world with dominant species used for the creation of the Ångström matrix.

Table 6.2. Location and period of data availability of operational AERONET stations in California.

Table 6.3 Name and location of the aircraft field campaigns and optical properties measured used in this work.

Table 6.4 Contingency matrix constructed from the aircraft measurements representing the percentage of aerosol sources from the ATOMFS classified into the different Ångström matrix classes.

Table 7.1 Derived values of OC AAE and OC contribution to wood smoke absorption of solar radiation as they depend on the chosen value of BC AAE.

Table 8.1 Comparison of spectral properties derived from AERONET observations and the GOCART model.

Table 8.2 Average AAOD for absorbing species at 550 nm in California determined from MISR and SSA_AERONET observations resolved by region and season.

Table 8.3 Radiative forcing of EC and carbonaceous aerosols determined at the TOA, surface, and within atmosphere column from the data assimilation scenarios in this work.

Table 9.1 CIMIS stations included in this analysis. All sites operational from (at least) November, 1986-December, 2011.

Table 9.2 Average change in surface clear sky flux between 1980-2009 based upon measurements from the CIMIS network.

Table 11.1 BC emissions in California based on various available sources.

Table 12.1 Average seasonal difference between WRF output and MERRA retrievals for short-wave solar flux at the surface and cloud optical thickness over California. WRF AOD was compared to MISR retrievals of AOD.

Table 12.2 Atmospheric heating and surface forcing from BC in Northern, Central, and Southern CA calculated off-line from WRF-Chem simulation. Upper and lower limits on uncertainty are given in parentheses.

Table 13.1 Change in atmospheric heating and surface forcing as a result of cutting BC emissions in half (indirect effects not included)

Table 13.2 The change in total downward short-wave flux at the surface as a result of reducing BC emissions by half.

LIST OF FIGURES

Figure 1.1 Trends in San Francisco Bay Area BC Concentration resolved by (a) day of week, (b) season, (c) year, and (d) estimated diesel emission factors.

Figure 1.2 Trans-oceanic and trans-continental BC aerosols represented by assimilated anthropogenic aerosol optical depth resolved by season.

Figure 2.1 Front panel and inside front panel of aethalometer and refurbished COH instrument. The refurbished COH instrument was equipped with a mass flow controller and data acquisition hardware (shown atop the instrument).

Figure 2.2. Comparison of two-hour average COH concentrations measured using the two field-bound refurbished monitors subject to soot from a methane-air flame.

Figure 2.3 Time series of COH and particle number concentrations measured with a condensation particle counter (CPC) during a laboratory evaluation of COH instrument performance. Both monitors sampled soot generated with a methane-air flame.

Figure 2.4 Scatter plot of average BC and COH concentrations measured in San Jose (March 2010 thru April 2011) and Vallejo (March 2010 thru March 2012).

Figure 3.1 A map of the U.S. indicating the states for which at least some COH records exist, and the nine states (in blue) for which we have determined annual BC trends.

Figure 3.2 (Left) Map of California showing where COH and EC were measured: IMPROVE sites operating between 2001 and 2005, and COH sites from 1980 to 2007. (Right) Graph showing the number of COH monitors in operation in California at least six months in any given year over the period 1970 to 2007.

Figure 3.3 Statewide average BC concentrations based on COH data sets obtained from CARB and EPA and distillate fuel oil (i.e., diesel fuel) consumption in California since 1960.

Figure 3.4 Average BC concentrations in California reconstructed from COH records resolved by air basin.

Figure 3.5 Statewide average BC concentrations in nine states in the U.S. with available COH records.

Figure 3.6 Annual cycles of BC concentrations by decade in California and New Jersey between 1960 and 2000.

Figure 3.7 Annual cycles of carbon monoxide emissions measured in several cities and modeled by Glen et al. (1996).

Figure 3.8 Weekly cycle of BC concentration by decade in California and New Jersey from 1960-2000.

Figure 3.9 Weekly cycle of BC concentration by decade in California air basins.

Figure 3.10 Distillate fuel oil consumption in California by sector, illustrating the portion of transportation distillate that is taxable (i.e., on-road) diesel.

Figure 3.11 Consumption of fossil fuel and biomass fuels in California. Note that energy consumption is plotted on a logarithmic scale.

Figure 3.12 Residual fuel oil consumption in California by sector.

Figure 4.1 Annual means of measured Black Carbon and BC fossil fuel emissions in California from 1985 to 2008 for the entire state, and by region in Southern (South of 35 N), Northern (North of 38 N), and Central California; and Annual means of measured Sulfate, Nitrate, and OC from IMPROVE network.

Figure 4.2 20-year average BC Concentration, rate of change of BC concentration, and rate of change of BC/non-BC aerosols from the IMPROVE network in California with measuring stations are indicated.

Figure 4.3 (Location of IMPROVE sampling stations in continuous operation from 1988-2007 in California, with annual means of measured BC, and average annual rate of change in mean BC concentration for IMPROVE sites with greater than 75% coverage in each time period.

Figure 4.4 Time series of measured BC/non-BC Aerosol ratio from the IMPROVE network in California and derived co-Single Scattering Albedo for visible light calculated using fixed absorption cross sections of $10.1 \times 10^{-6} \text{ m}^2 \text{ mg}^{-1}$ and $7.5 \times 10^{-6} \text{ m}^2 \text{ mg}^{-1}$.

Figure 4.5 Monthly averaged SSA calculated from measurements and retrieved from the AERONET network in California from 1988-2010.

Figure 4.6 Annual mean measurements from the South Lake Tahoe (SOLA) station in California for (a) OC and EC absolute concentrations and (b) EC/OC and K/EC ratios.

Figure 4.7 Annual mean measurements of (a) EC and (b) non-EC aerosols from the EPA-STN network in California that represents limited urban measurements.

Figure 5.1 Normalized frequency distributions for the Scattering Angstrom Exponent (440-675 nm), Absorption Angstrom Exponent (440-675 nm), Absorption Angstrom Exponent (675-870 nm), and AAE2/AAE1 ratio measured at DU, BB, UF, and NF AERONET sites.

Figure 5.2 Scatter plots of AAE1 and EAE1 calculated from AERONET measurements at (a) DU, (b) BB, (c) UF, (d) NF, and (e) CA sites.

Figure 5.3 Mean value of AAE1 determined by averaging the frequency distribution for selected AERONET sites.

Figure 5.4 Normalized frequency distribution of the OC absorption Angstrom exponent determined from BB, CA, NF, and UF sites between 440 and 675 nm.

Figure 5.5 Calculated SSA value at 675 nm for EC, OC, and Dust using AERONET stations segregated into source regions.

Figure 5.6 The calculated AAE1 for the total aerosol as a function of AOD at 440 nm and 675 nm, and the measured SSA at 440 nm and 675 nm from selected AERONET site.

Figure 5.7 Calculated AAE1 for the total aerosol as a function of AOD at 440 nm, and measured SSA at 440 nm from selected AERONET sites.

Figure 5.8 Species resolved AOD, AAOD, and emissions in California for EC, OC, and dust. Also illustrated is the wavelength dependent relative absorption of OC and EC.

Figure 5.9 Fraction of AAOD in CA attributed to dust, OC, and EC at 440 nm as a function of AAE and EAE/SAE

Figure 5.10 Comparison of AAOD from CA sites directly measured from AERONET and reconstructed from equation 5.4 at 440 nm, 675 nm, and 870 nm

Figure 6.1 Division of the Absorption Ångström Exponent vs. Scattering Ångström Exponent space, the Ångström matrix, overlapped with the AERONET measurements from stations with a dominant species (fossil fuel, biomass burning or dust).

Figure 6.2 Location of flight paths of the aircraft campaigns and the AERONET stations used for relating absorbing aerosols to emission sources.

Figure 6.3 Estimated contribution to light absorption derived from AERONET stations in California separated by region and season: (Northern vs. Southern California and winter/spring vs. summer/autumn).

Figure 6.4 Representative ATOFMS spectra for different aerosol sources including primary fossil fuel, secondary fossil fuel, primary biomass burning, secondary biomass burning, and dust.

Figure 6.5 Overall chemical composition detected with the ATOFMS in the three aircraft campaigns conducted in California: CalNex, CARES, and CalWater.

Figure 6.6 Absorption Ångström Exponent vs. Scattering Ångström Exponent scatter plot of in situ aircraft measurements in California; the color code represents the dominant aerosol source detected with the ATOFMS for each measurement. Also shown is a frequency histogram of the Absorption Ångström Exponent for each aerosol source.

Figure 7.1 Estimated contributions of black and organic carbon to the spectral attenuation of a residential wood smoke particulate matter sample.

Figure 7.2 Histograms of absorption Ångström exponents computed over the 360 to 700 nm spectral range.

Figure 7.3. Fraction of solar radiation absorbed by organic carbon rather than black carbon in residential wood smoke particulate matter.

Figure 8.1 Operational AERONET sites in California and neighboring states, indicating availability of valid quality assured measurements.

Figure 8.2 Average MISR satellite retrievals of the total AOD, total AAOD, EC AOD, and EC AAOD for the months of June-August in the California domain.

Figure 8.3 Seasonally averaged values of the SSA from GOCART and AERONET at 440 nm, 670 nm, and 870 nm. The wavelength dependence of all available SSA measurements is also illustrated.

Figure 8.4 Relative contributions to the AAOD (550 nm) from dust and carbonaceous aerosols calculated using MISR AOD and SSA_AERONET, MISR AOD and SSA_GOCART, and GOCART simulations

Figure 8.5 Relative contributions to the AAOD (550 nm) from EC and OC calculated using MISR AOD and SSA_AERONET, MISR AOD and SSA_GOCART, and GOCART simulations

Figure 8.6 Comparison of simulated AOD and AAOD for carbonaceous aerosols from the GOCART and WRF models with the observationally constrained approach followed in this study.

Figure 8.7 Seasonally and spatially resolved vertical profiles of aerosols in California constructed from CALIPSO satellite retrievals. Aerosol extinction is directly correlated to aerosol mass loading.

Figure 8.8 Atmospheric heating due to carbonaceous aerosols (EC+OC) in California calculated using observationally constrained data, GOCART simulations, and WRF simulations.

Figure 8.9 Radiative forcing at the (a) Top-of-Atmosphere (TOA), (b) in the Atmosphere (atm), and (c) at the surface (sfc) attributable to dust and carbonaceous aerosols in California determined using observationally constrained aerosol properties.

Figure 8.10 Top of the Atmosphere forcing for EC and Carbonaceous aerosols determined in the bounding cases using SSA_AERONET and SSA_GOCART in California.

Figure 8.11 Change in the radiative forcing due to carbonaceous aerosols as a consequence of a 50% reduction in EC aerosol loading in California between 1980-2000.

Figure 9.1 Location of sites in the CIMIS network in California that provide solar flux data in the decades between 1980-2010.

Figure 9.2 Monthly averages of surface solar flux in California obtained from the CIMIS network. A large summer-winter variability is observed.

Figure 9.3 Diurnal variations in surface flux measured at the Davis station in (a) June and (b) December. Large deviations from the upper envelope indicate the influence of clouds.

Figure 9.4 Histogram of surface flux measurements at the (a-b) Davis and (c-d) Riverside stations in (a,c) June and (b,d) December. The second (higher) mode represents clear-sky flux.

Figure 9.5 Trends in the clear-sky daytime surface flux measured by the CIMIS network for (a,c) summer months and (b,d) winter months, in (a-b) Northern and (c-d) Southern California.

Figure 12.1 Seasonal mean mass concentrations of speciated $PM_{2.5}$ such as EC, OM, dust, sulfate, nitrate, ammonium, sea salt, and unspicated $PM_{2.5}$ from IMPROVE and EPA measurements and the corresponding WRF-Chem simulations over California in 2005. The right-bottom panel shows the results from WRF-Chem sensitivity simulation with anthropogenic EC emissions doubled.

Figure 12.2 Spatial distributions of seasonal mean 550 nm AOD and AAOD from the WRF-Chem simulations with anthropogenic EC emissions doubled over California in 2005. The numbers represent the four AERONET sites: 1-Trinidad Head; 2-Fresno; 3-UCSB; 4-Tonopah Airport.

Figure 12.3 Seasonal variations of total 550 nm AOD and AAOD and their contributions from sulfate, OM, EC, dust, and other species from the WRF-Chem simulations with anthropogenic EC emission doubled. Other species include nitrate, ammonium, sea salt, and unspiciated PM_{2.5}.

Figure 12.4 Spatial distributions of seasonal mean aerosol direct radiative forcing at the top of atmosphere (TOA), in the atmosphere (ATM), and at the surface (BOT) from the WRF-Chem simulations with anthropogenic EC emissions doubled over California in 2005. At TOA and BOT, positive value represents downward radiation; in ATM, positive value represents warming.

Figure 12.5 Seasonal variations of aerosol direct radiative forcing and its contributions from sulfate, OM, EC, dust, and other species at the TOA, in the atmosphere, and at the surface from the WRF-Chem simulations with anthropogenic EC emission doubled.

Figure 12.6 WRF surface temperature compared to CIMAS measurements for summer and winter seasons.

Figure 12.7 WRF precipitation compared to CIMAS measurements for summer and winter seasons.

Figure 12.8 Comparison of WRF-Chem-predicted surface concentrations of EC with measured EC concentrations from IMPROVE and EPA networks for summer and winter.

Figure 12.9 Comparison of WRF-Chem-predicted surface concentrations of PM_{2.5} with measured PM_{2.5} concentrations from IMPROVE and EPA networks for summer and winter.

Figure 12.10 Modeled SW surface flux vs. the off-line, calculated SW surface flux.

Figure 12.11 Contribution of BC to total atmospheric heating due to aerosol absorption as a function of altitude.

Figure 13.1 Changes in all-sky net solar radiation at the surface (in W m⁻²) comparing simulations for the 2000s (2xEC) to the 1960s (10xEC).

Figure 13.2 Left: Changes in diabatic heating comparing the simulation for the 2000s with the 1960s (in K/day). Right: Similar to the left but for changes in atmospheric temperature (°C).

Figure 13.3 Changes in 2-meter surface temperature comparing the 2000s to the 1960s in °C.

Figure 13.4 Comparison of observed (solid) and simulated (dashed) temperature profiles averaged over three sounding locations in CA (OAK, VGB, NKX) for four seasons for 2005.

Figure 13.5 (a) Percent reduction in BC concentration as a result of cutting BC emissions in half, and (b) the associated change in atmospheric heating as a function of altitude.

Figure 13.6 The change in cloud optical thickness in (a) Summer and (b) Winter as a result of reducing baseline BC emissions by half.

LIST OF ACRONYMS

| | |
|---------|--|
| BC | Black Carbon |
| EC | Elemental Carbon |
| OC | Organic Carbon |
| BrC | Brown Carbon (Absorbing Fraction of OC) |
| ATOFMS | Aerosol Time of Flight Mass Spectrometry |
| GCM | General Circulation Model |
| AERONET | Aerosol Robotic Network |
| MISR | Multi-angle Imaging Spectro Radiometer |
| COH | Coefficient of Haze |
| AQMD | Air Quality Management District |
| AAE | Absorption Angstrom Exponent |
| SAE | Scattering Angstrom Exponent |
| EAE | Extinction Angstrom Exponent |
| SSA | Single Scattering Albedo |
| TOA | Top Of Atmosphere |

ABSTRACT

This report provides an assessment of the impact of black carbon on the regional radiative forcing and climate trends of California. The present regional integrated assessment is the first such attempt to estimate the radiative forcing of BC for one region (California in this case), both from a bottom-up approach (starting with emission inventory as input to aerosol-transport models) and a top-down approach (adopting satellite data in conjunction with ground based column averaged aerosol optical properties). This approach enabled us to uncover three unanticipated major findings: i) The first finding concerns the large decadal trends in BC concentrations largely in response to policies enacted to decrease PM emissions from diesel combustion. ii) The second is the discovery of the large effects of brown carbon (a form of organic carbon aerosols) on radiative forcing. iii) The third is the large discrepancy between the top-down and the bottom-up approach of estimating radiative forcing and ways to close the gap.

Observed multi-decadal BC trends: The trends in BC concentrations were determined from assimilation of mass-based measurements (from the IMPROVE network that typically samples remote areas), and from analysis of the large set of available COH (Coefficient of Haze) measurements (which typically sample urban areas). The more reliable IMPROVE data showed that the annual average BC concentrations in California have decreased by about 50% from $0.46 \mu\text{g m}^{-3}$ in 1989 to 0.24mgm^{-3} in 2008. The COH data revealed that BC concentrations in California decreased markedly from about $3.9 \mu\text{g m}^{-3}$ in 1966 to $2.3 \mu\text{g m}^{-3}$ in 1980 to $1.1 \mu\text{g m}^{-3}$ in 2000, agreeing with the trends reported from the IMPROVE data sets. Trends in other co-emitted aerosols such as OC, sulfates were much smaller or statistically insignificant. BC trends are related to an order of magnitude reduction in diesel PM emissions since the first smoke reduction standards were introduced in the 1970s. Other determining factors likely include BC emissions reduction from other sources in the transport sector, the cleanup of BC emissions in the industrial sector, and decreasing wood and waste burning since 1990. *Observations of large negative trends in BC and the lack of corresponding negative trends in co-emitted OC and sulfate aerosols gives compelling observational support to the conclusion of Jacobson (2010) and Bond et al (2013) that mitigation of diesel BC would mitigate global warming.*

Importance of Brown Carbon for Solar absorption: Analysis of the spectral dependence of solar absorption measured in-situ as well as over the column indicates an enhanced absorption at shorter (<500 nm) wavelengths that deviates from the expected behavior of BC. This enhanced absorption is attributed to organic, "brown", carbon. The solar absorption due to brown carbon is found to contribute as much as 40% of the BC forcing in the near-UV (<440 nm) wavelengths. Field measurements in several independent campaigns using aethalometers for absorption, and the ATOFMS for detailed chemical analysis find that brown carbon is primarily related to residential wood burning. However, a new class of particles related to secondary organics, i. e., aged large organic particles, is also found to contribute to solar absorption, thus raising the possibility that fossil fuels also contribute – via their contribution to secondary

organic particles – to brown carbon absorption. *We find that the direct warming effect of brown carbon, ignored in most models, offsets about 60% to 90% of the direct cooling effects of other organic carbon aerosols.*

Direct Radiative Forcing Over California: We determine the radiative forcing using a top-down approach developed by the PI's (VR) group that relies on NASA's ground based AERONET data and assimilated satellite measurements (MISR) of aerosol optical properties. This observationally constrained top-down (OC_TD) estimate includes solar absorption by brown carbon while the emission inventory based bottom-up (EI_BU) estimates included in this study do not account for brown carbon. The uncertainty in the OC_TD forcing is about $\pm 40\%$. For the annual mean, the current top-of-atmosphere (TOA) forcing of BC+OC varies from about 0.2 Wm^{-2} over Northern California (NCA) to as large as 1.9 Wm^{-2} over Southern California (SCA). The implication is, in the 1980s when BC concentrations were higher by about 100%, the TOA forcing for BC+OC could have been as large as 0.4 to 3.8 Wm^{-2} . *Overall we conclude that the large negative trend in BC radiative forcing and the lack of corresponding negative trends in OC, confirms the assessment of some other studies (Jacobson, 2010 and Bond et al, 2013) that diesel related BC emission reduction would lead to global cooling.*

Regional Climate Effects: The regional climate changes associated with the observed reduction in BC concentrations were estimated with a regional climate model. *The declining trends in BC (by a factor of five to approximate the 1960s) cause a reduction in the TOA direct radiative forcing everywhere and the cooling effect ranges from -0.5 to -3.5 Wm^{-2} , consistent with the OC_TD estimates, with larger effects during summer than winter.* In response to this change, the lower atmosphere is found to cool everywhere, accompanied by a smaller warming near the surface, which is not statistically significant in any season. Overall, the local climate effects are small.

Primary Finding: Mitigation of Global Warming

Reductions in emissions of BC mostly from diesel engines, since the 1980s have contributed significantly to mitigation of global warming, equivalent to mitigation of 21 million metric tons of CO_2 emissions annually. This climate benefit may date back to at least the 1960s, and is currently ongoing.

Because of the long lifetime of CO_2 (one century or longer) compared with the much shorter lifetime of BC (about one week), mitigation of CO_2 is critical for limiting long term (>50 years) global warming, while mitigation of BC is critical for limiting near-term (<50 years) warming.

EXECUTIVE SUMMARY

OVERALL FINDING

BC emission reductions since the 1980s, attributed in large part to diesel engine emissions mitigation, are equivalent to *reducing CO₂ emissions by 21 million metric tons annually. This is approximately equal to 5 % of the total direct CO₂ annual emissions of 393 million metric tons.*

As on-road diesel is very low in sulfur in developed regions and lowering elsewhere, and since compared to other major BC sources, diesel PM has more BC and less OC, it follows that controlling diesel BC would have a cooling effect. The control of BC from diesel therefore is an effective means of mitigating near-term global climate change. This conclusion is consistent with findings of recent studies [Jacobson, 2010; Bond *et al.*, 2013], which conclude that reduction of BC from diesel sources would lead to global cooling. However, we would like to caution that, without simultaneous reduction of CO₂ emissions, it will not be possible to limit future warming to below 2°C as required by the Copenhagen accord.

Background

Black Carbon (BC): Soot contains black carbon and organic carbon aerosols, which absorb and scatter solar radiation and thus impacts the climate system from local to regional and global scales. The component of soot that absorbs solar radiation is usually referred to as black carbon (BC) or elemental carbon (EC). The two terms, BC and EC, are used interchangeably and we follow the same practice in this report. BC or EC is simply a functional definition that depends on the measurement technique. In principle, the relatively strong light absorption properties of BC can be used to infer BC from an optical measurement and knowledge of the mass specific absorption of BC. In thermal methods, the filter media used for sample collection is heated and the thermally evolved carbon in the specified temperature plateau and analysis atmosphere defines the concentration of EC and organic carbon (OC).

Brown Carbon (BrC): Organic carbon is normally assumed to be a pure scattering aerosol. However, recent experimental studies have demonstrated that a fraction of OC also absorbs sunlight with their absorption increasing dramatically towards shorter wavelengths (<500 nm wavelengths). The absorbing part of OC referred to as brown carbon. In this report, the term OC includes BrC.

Radiative Forcing: The net effect of absorption and scattering of solar radiation by, BC and OC, is to alter the solar radiation absorbed by the surface and the atmosphere, which is the fundamental driver of the global climate system. The

change in the radiative heating of the climate system is referred to as the ‘Radiative Forcing’ [see the primer on radiative forcing later in the summary]. The change in the forcing due to scattering and absorption of solar radiation is referred to as ‘Direct Forcing’. But the addition of BC and OC aerosols as well as the alteration of solar heating by BC and OC alters the cloud fraction and cloud properties, which in turn alters the radiative forcing since clouds are the largest modulators of solar radiation. These cloud induced radiative forcings are referred to as indirect and semi-direct forcings [see the primer]. These changes to the solar radiative forcing [units of $W m^{-2}$] are the primary metric used to assess the importance of BC and OC on climate.

Motivation [BC is the second Largest Contributor to Global Warming]: Black carbon (BC), the main light-absorbing component of soot is the principal absorber of visible solar radiation in the atmosphere. *Jacobson, [2002]* and *Ramanathan and Carmichael [2008]* concluded that BC is the second largest contributor to global warming, next to CO_2 . For present day BC, due to both natural and anthropogenic sources, Ramanathan and Carmichael estimated a direct forcing of $0.9 W m^{-2}$ [0.45 to $1.35 W m^{-2}$] compared to $1.6 W m^{-2}$ for CO_2 [*Forster et al., 2007*] - this conclusion was debated because most estimates of forcing from models were a factor of two to three lower. A major landmark study of the BC forcing problem was published this year [*Bond et al., 2013*] by a group of researchers that included many modeling groups, and their estimate of $0.88 W m^{-2}$ for the BC direct forcing (due to all BC sources) is nearly identical to Ramanathan and Carmichael’s estimate of $0.9 W m^{-2}$. Because of its short life times of few weeks, BC is concentrated close to the sources and hence a regional evaluation is critical for a better understanding of the global effects. Furthermore, California has witnessed major decreases in its BC concentrations and we need to understand the impact of these regional trends in climate.

The unique integrated approach

We have developed a balanced approach between observations, data analyses, and modeling studies, allowing us to uniquely constrain the estimates provided in this study using measurements conducted by ground based network, aircraft and satellite instruments. The study consisted of four primary components (i) analysis of available measurements, and documentation of multi-decadal BC trends constrained by field measurements, (ii) estimation of the direct aerosol forcing due to black and brown carbon using integrated observations as well as models, (iii) source apportionment based upon chemical mixing state, and (iv) estimating the climate impact of BC emissions under various mitigation scenarios. The full climate impact of BC on the regional climate of California is evaluated by using regional climate models in a series of numerical experiments with varying BC emissions to determine changes in the surface temperature and hydrology. The regional climate models used to evaluate the climatic impacts of BC are also used in step (ii) to estimate the BC forcing, so their uncertainty can be assessed by comparing their estimated BC forcing with the observation based estimates. Statewide temporal and spatial resolved BC concentrations have been derived

by analyzing the coefficient of haze [COH] (directly correlated to the BC) recorded at 100 locations throughout California (data available from CARB). A key component of this work involves determining the actual single particle mixing state of soot particles in California. These measurements allow us to proceed without making major assumptions regarding the size, mixing state, and optical properties of ambient soot particles that have resulted in tremendously large uncertainties in prior studies. The details of our unique approach are given in the Methods section at the end of this section.

Principal Findings

I. BC concentration results

We examine the temporal and the spatial trends in the concentrations of black carbon (BC) using filter based mass measurements recorded by the IMPROVE monitoring network, and optical measurements reconstructed from the available Coefficient of Haze (COH) records in California.

- 1. Annual average BC concentrations measured at California IMPROVE sites have decreased by about 50% from $0.46 \mu\text{g m}^{-3}$ in 1989 to $0.24 \mu\text{g m}^{-3}$ in 2008 compared to a corresponding reductions in diesel BC emissions (also about 50%) from a peak of 0.013 Tg Yr^{-1} in 1990 to 0.006 Tg Yr^{-1} by 2008 (Figure 2(a)).*
- 2. A larger set of COH measurements is also used to determine BC concentrations and reveals that these trends are uniform across the state and persistent in several major air basins (Figure 2(b)).*

The consistency between the IMPROVE and COH trends is important since the COH data are largely from urban sites whereas IMPROVE is from remote sites.

- 3. A corresponding trend in co-pollutants such as nitrates, sulfates, and organic carbon is not observed (Figure 2(a)).*

This finding is crucial, since the co-pollutants are largely cooling aerosols, through their direct and indirect effects on clouds. Since they are not showing negative trends, it implies that the decrease in BC will most likely lead to a global cooling effect from California's BC reductions.

- 4. As no similar trends are observed in other chemical source tracers (such as K, for biomass burning), we therefore attribute the observed BC trends primarily to the emission reduction from transport-related PM emissions, primarily from diesel.*

A detailed analysis of technology based emission inventories and fuel use in California indicates that although the total consumption in diesel fuel has

increased, the emissions of BC from diesel fuel combustion have decreased significantly. The reduction in emissions is due to a number of factors, including the introduction of low sulfur fuel, tighter emission standards, cleaner burning engines, and other improvements in technology mandated by statewide regulations. California therefore appears as a success story in mitigating the anthropogenic impact on climate. While, decreasing trends in BC have been noted in other states (of US), we are unable to comment on their climate mitigation efficacy since data on other co-pollutants have not been analyzed in published literature.

5. Our conclusion that the reduction in diesel emissions is the primary cause of the observed BC reduction is also substantiated by a significant decrease in the ratio of BC to non-BC aerosols.

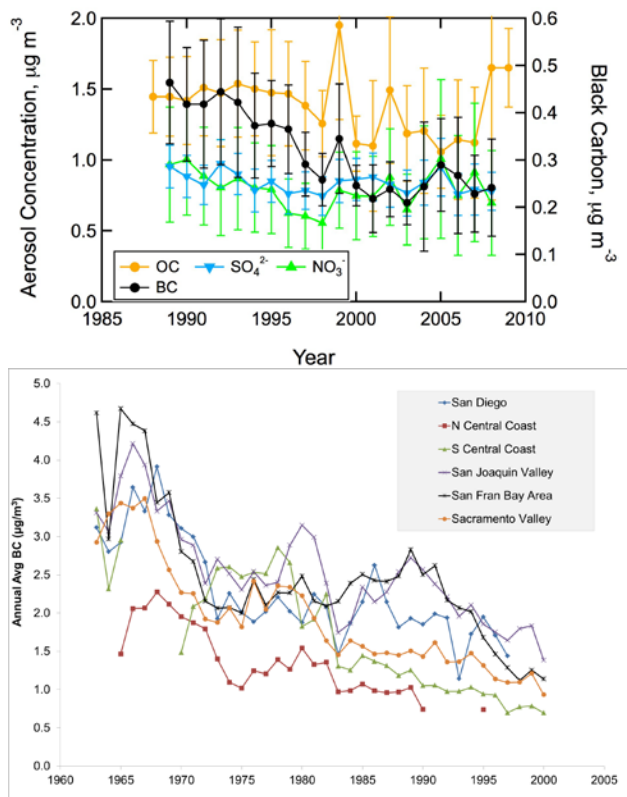


Figure 0.1 (a) Statewide trends in concentrations of common aerosol species from the IMPROVE network, and (b) historical BC concentrations resolved by air basin. A clear reduction in BC is observed.

II. Role of brown carbon absorption

We have developed an observationally based analytical method for rigorously partitioning measured aerosol absorption optical depths (AAOD) and single scattering albedo (SSA) among EC and BrC using multi wavelength measurements of total (EC, OC and Dust) absorption.

1. We have quantified column-integrated absorption in multiple wavelengths by brown carbon from observations for the first time.

The new method we developed separates dust, BC and BrC absorption from spectral solar observations. It can now be applied to other regions of the world.

2. Organic carbon (OC) is shown to absorb strongly at visible to UV wavelengths, an effect typically not represented in climate models. The BrC absorption at 440 nm is about 40% of the EC, while at 675 nm it is less than 10% of EC (Figure 2).

We find an enhanced absorption due to BrC in the summer months, and in South California (related to forest fires and secondary OC). The contribution of BrC to the total aerosol absorption is largest over northern and central California.

3. BrC emissions are likely both from biomass burning (forest fires and residential wood burning) as previously thought, and also from large aged particles indicating that secondary organics may also be absorbing.

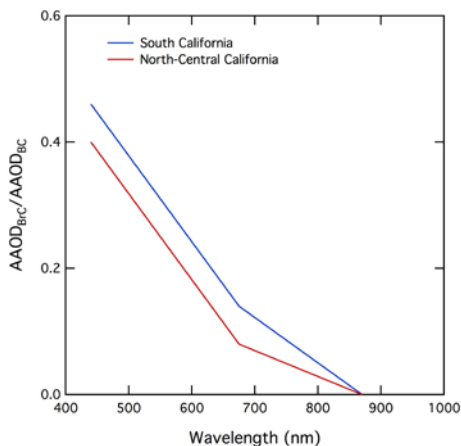


Figure 0.2 Wavelength dependent relative Absorption Aerosol Optical Depths (AAODs) for BC and BrC determined from ground-based estimates of the SSA and AOD in California.

Formatted: Numbered + Level: 1 + Numbering Style: 1, 2, 3, ... + Start at: 1 + Alignment: Left + Aligned at: 0.25" + Indent at: 0.5"

Formatted: Numbered + Level: 1 + Numbering Style: I, II, III, ... + Start at: 1 + Alignment: Left + Aligned at: 0.25" + Indent at: 0.75"

III. Source Attribution and Speciation

1. Major differences exist in the PM sources in northern and southern California. In-situ measurements of optical properties and chemical mixing state reveal fossil fuel sources contribute the most strongly in southern California, whereas biomass burning and biogenic sources dominate in northern California. This has been shown in other recent studies as well (Cahill et al. 2012).

2. Using optical properties for estimating aerosol speciation using satellites or networks such as AERONET has the potential to provide extensive input into global climate and air pollution studies. This study demonstrates that the interpretation of the AERONET results is strengthened by complementary measurements of aerosol sources.

Speciation of dust, BC and BrC, are well classified by optical data, but the separation between fossil fuel and biomass burning sources has limitations because of their overlapping optical properties.

3. Despite these limitations, detailed comparison reveals the significance of aerosol absorption due to secondary organic aerosol (OC) which is currently underestimated in climate models, in addition to black carbon. Brown carbon and secondary sources impact many absorption events, indicating these processes must be given consideration when developing future climate mitigation policies.

Formatted: Font: 12 pt, Bold

Formatted: Font: (Default)
Arial, 12 pt, Italic

Formatted: Numbered + Level: 1
+ Numbering Style: 1, 2, 3, ... +
Start at: 1 + Alignment: Left +
Aligned at: 0.25" + Indent at:
0.5"

Formatted: Font: (Default)
Arial, 12 pt

Formatted: Font: (Default)

Formatted: Numbered + Level: 1
+ Numbering Style: 1, 2, 3, ... +
Start at: 1 + Alignment: Left +
Aligned at: 0.25" + Indent at:
0.5"

Formatted: Font: (Default)
Arial, 12 pt, Italic

Formatted: Font: Italic

Formatted: Font: (Default)
Arial, 12 pt, Italic

Formatted: Font: Italic

Formatted: List Paragraph, No
bullets or numbering

Formatted: Font: (Default)

Formatted: Font: (Default)

Formatted: Font: (Default)

Formatted: Font: (Default)
Arial, 12 pt, Italic

Formatted: Numbered + Level: 1
+ Numbering Style: 1, 2, 3, ... +
Start at: 1 + Alignment: Left +
Aligned at: 0.25" + Indent at:
0.5"

Formatted: Font: Italic

Formatted: Font: (Default)
Arial, 12 pt, Italic

III.IV. Radiative forcing results: Present day values

Radiative Forcing: A Primer

Direct Radiative Forcing: BC and OC increase the amount of solar radiation absorbed by the atmosphere, by intercepting the direct incoming solar radiation and also by intercepting the solar radiation reflected by the surface, the atmosphere and the clouds. The interception of solar radiation also leads to a decrease in solar radiation absorbed at the surface (dimming). The alteration of the solar absorption of the surface and the atmosphere by BC and OC is referred to as *direct radiative forcing*. The net effect is the sum of the atmospheric heating and the surface dimming and is referred to as the top-of-the atmosphere (TOA) forcing. The TOA forcing is the most relevant quantity for assessing the significance of California's BC policy actions for mitigating global warming. However, for assessing the impacts on California's regional climate, we have to examine the impact of EC and OC on atmospheric solar heating (atmospheric forcing) and surface solar dimming (surface forcing).

Indirect and semi-direct Radiative Forcing: BC and OC also influence cloud formation. They nucleate cloud drops that increase the number of cloud drops and also increase cloud fraction, both of which enhance the cloudy-sky albedo and lead to cooling. This is the indirect effect of BC and OC. On the other hand, the solar heating of the atmosphere by BC and BrC leads to burn-off of clouds. In addition, inclusion of BC in cloud drops also enhances solar absorption by the drops. This cloud-inclusion effect also enhances cloud burn-off. The burn-off in turn decreases the cloudy-sky albedo and thus provides an offset to the cooling effect of the indirect effect.

The annual average direct radiative forcing associated with BC+OC from the observationally constrained Top-Down (OC_TD) approach, initialized with two assimilated data sets is summarized in Table 1. The total aerosol optical depth (AOD) is retrieved from the MISR satellite whereas the single scattering albedo (SSA) is based upon observations from the AERONET network, and from the GOCART climate model. The two different values of SSA allow us to estimate the upper and lower limits for the BC and BrC (details in Chapter 9). However, our baseline estimate is that given by the version of OC_TD with SSA from AERONET. Table 1 also shows simulated forcing by the emission-inventory based bottom up (EI_BU) WRF-Chem models. PNNL and LBL refer to the two modeling groups participating in our study.

1. *Direct Radiative Forcing by BC+OC is positive everywhere in California. It ranges from 0.2 Wm^{-2} in northern California to 0.88 Wm^{-2} over S. California.*

- 2. The annual average BC+OC direct forcing for California estimated using the WRF-Chem regional climate model (with the published emission inventory) is 0.16 W m^{-2} , compared to 0.51 W m^{-2} ($\pm 40\%$) from the observationally constrained estimate. Thus, even regional models with region specific emissions, severely underestimate the BC+OC warming effects by a factor of three.*

The WRF-Chem model also underestimates surface BC concentrations by a factor of two. We show the forcing with BC emissions increased by a factor of 2 (4th column) that reduce this discrepancy, but the model forcing of 0.29 W m^{-2} is still much lower than the OC_TD approach. Some of the remaining discrepancy can be further explained due to the neglect of BrC absorption in the regional models.

- 3. The underestimation (by a factor of three) is consistent with Bond et al. [2013]'s conclusion that models underestimate absorption by BC by a factor of three on a global mean basis.*
- 4. The BrC absorption has a major impact on the direct forcing due to OC aerosols. Without BrC absorption, models estimate direct forcing due to OC to be between -0.30 and -0.15 W m^{-2} depending on the location and region, whereas inclusion of BrC brings the net cooling down to between 0.00 and -0.10 W m^{-2} . Thus models that neglect BrC severely overestimate the OC cooling effects.*

Table 2 presents a comparison in the atmospheric heating rates from the observationally constrained calculations, and the WRF-Chem regional model operating in two independent configurations. All three calculations produce similar trends in the magnitude of the forcing. This agreement obtained from three independent calculations indicates the robustness and significance of the results.

- 5. The atmospheric heating, or energy added to the atmosphere, is a factor of four to eight larger than the TOA forcing (Table 2).*

Carbonaceous aerosols are found to be warming in all regions and seasons with a magnitude ranging between 0.5 and 3.5 W m^{-2} . The greatest warming is observed in Southern California (which typically has a higher anthropogenic aerosol concentration and lower cloud cover), and also in the summer (possibly due to a higher net solar flux).

| | <u>Observationally Constrained Top-Down</u> | | <u>Emission Inventory Based Bottom-Up</u> | |
|--|---|--------------------|---|--------------------|
| | (OC TD) | | (EI BU) | |
| | SSA from AERONET | SSA from GOCART | WRF_PNNL (1*BC) | WRF_PNNL (2*BC) |
| TOA forcing | | | | |
| North | 0.20 | 0.28 | 0.09 | 0.16 |
| Central | 0.44 | 0.48 | 0.17 | 0.32 |
| South | 0.88 | 1.92 | 0.21 | 0.40 |
| State | 0.51 | 0.89 | 0.16 | 0.29 |
| Atmospheric heating, W m⁻² | | | | |
| North | 1.73 | 1.79 | 0.60 | 0.82 |
| Central | 2.40 | 2.78 | 0.86 | 1.25 |
| South | 2.44 | 4.05 | 0.96 | 1.41 |
| State | 2.19 | 2.87 | 0.81 | 1.16 |
| Surface forcing, W m⁻² | | | | |
| North | -1.54 | -1.47 | -0.51 | -0.65 |
| Central | -1.94 | -2.38 | -0.68 | -0.92 |
| South | -1.62 | -2.47 | -0.75 | -1.01 |
| State | -1.70 | -2.11 | -0.65 | -0.86 |

Table 0.1 Annual average radiative forcing attributed to BC+OC at the top of the atmosphere, atmospheric heating, and at the surface determined using the observationally constrained MACR model and the WRF-Chem climate model simulations based on emission inventories.

IV-V. Surface Brightening:

Radiative calculations also estimate that the 50% decrease in BC concentration from the 1980s to current levels should have led to an increase in the surface solar radiation (surface brightening) between 1.5-3.5 W.m⁻².

We looked for this brightening effect in a network of surface solar radiometers operated by California's CIMIS network since 1982. The inter-annual variability was much larger than the detected trend in solar flux measurements and when this is considered with the limited data duration of the measurements (about 25 years), we are led to the deduction that the detected trends during the 1980s to 1990s are not statistically significant to verify the predicted brightening trends due to decreasing BC concentrations.

V.VI. Implication to mitigation of global warming

1. *Our findings thus far suggest that policies enacted by California to reduce diesel emissions should have led to a substantive mitigation of global warming.*

This conclusion is derived from the following observations and model simulations:

2. *The observed decrease in surface-BC by a factor of 2 from 1989 to 2008 and by a factor of 3.5 from 1960s to 2008.*

3. *This decrease was not accompanied by a comparable decrease in OC or other cooling aerosols such as sulfates.*

4. *As a result the decrease of BC was accompanied by a decrease in ratio of BC to Non-BC aerosols, which implies the warming aerosols decreased more in relation to cooling aerosols.*

6. *The observed BC decreases were largely attributed to the decrease in diesel emissions of BC.*

7. *Targeted emission controls adopted by the State of California are shown to be effective in reducing BC concentrations, by a factor of at least 2 dating back to the 1980s, and by as much as a factor of 3.5 dating back to the 1960s. At the regional level this decrease is associated with a TOA cooling of between 0.5 and 1.5 W m⁻².*

8. *The indirect and semi-direct forcing changes due to the observed decrease in BC is expected to be much smaller than the direct forcing changes given above, due to the following two reasons: The negative indirect forcing is large mainly for OC and we did not observed statistically significant changes in OC concentrations (as expected for diesel related BC changes); As estimated by UNEP(2011) and Bond et al (2013), the sum of the indirect effect and the semi-direct effect is nearly zero for BC.*

The above finding, while it is the most important scientific aspect of our results, need to be validated by doing similar analyses for other states of US which have experienced strong reductions in BC.

In order to estimate the global warming mitigation from this diesel related BC forcing decrease, we need to account for not only the direct radiative forcing due to BC but also the following: Brown Carbon absorption; indirect effects of BC and OC; cloud-inclusion effects of BC and BrC; semi-direct effects of BC and BrC. We are aware of only one such modeling study by Jacobson (2010) which has explicitly estimated the global warming potential of fossil fuel BC. Furthermore, Jacobson's direct forcing estimate is consistent with our OC_TD estimates. As a result, we rely on Jacobson's 100 Year-GWP, which for fossil BC is 3000 (using his lower range).

9. *We estimate that reduction of BC emissions primarily from diesel engines from 1989 to 2008 has mitigated global warming equivalent to reducing annual CO₂ emissions by 21 million metric tons/year. This corresponds to about 5% of California's 2009 CO₂ direct emissions of 393 metric tons.*

VI.VII. Validation and Improvement of regional climate model treatment of BC forcing

Our goal is to use Emission Inventory based bottom-up (EI_BU) regional models to understand the regional climate effects of BC mitigation measures. However, we must validate these models first. In this study, we use the WRF-Chem model in a variety of numerical experiments to estimate the seasonal scale changes in radiative forcing. Two configurations of the WRF-Chem model were used, the standard version 3.2.1, and one that includes more updated cloud microphysical and radiative transfer parameterizations [Zhao *et al.*, 2012].

1. *A comparison between the simulated BC concentration and measurements at over 30 sites in California revealed that WRF-Chem under-predicted BC by nearly a factor of two, which indicates that the emission inventory developed in the ARCTAS-CA campaign may be under representing BC.*

The climate impact of BC was evaluated by changing the emissions by factors of 10x, 5x, and 2x. The 2x case approximates the conditions for the present day emissions; the 5x and the 10x cases approximate the emissions during the 1980s and the 1960s respectively.

2. *The simulated seasonal and regional variation in BC forcing is consistent with the patterns in OC_TD and furthermore, in agreement with OC_TD, the TOA forcing is positive everywhere. However, the direct forcing of (BC+OC) even with the 2x simulations is about 60% smaller than the OC_TD values.*

Table 2 compares the atmospheric heating calculated using both the observationally constrained and climate model approaches. Two sets of observationally constrained calculations were performed – in the first, OC was

treated as a scattering species, and in the second, some of the OC was allowed to absorb light as well as the BC.

3. *The comparison indicates that about a third of this difference between the models and the observationally constrained approach is due to the fact that the models ignore BrC. With respect to the other 2/3, we must point out that the observational estimates have an uncertainty of ±40%.*

| | | Observationally Constrained BC Only | Observationally Constrained BC+OC | WRF-CHEM calculation using 2xBC emission: PNNL | WRF-CHEM calculation using 2xBC emission: LBL |
|-------------------|---------|---|---|--|---|
| Annual Average | North | 1.36 | 1.54 | 0.82 | 0.99 |
| | Central | 2.10 | 2.26 | 1.25 | 1.31 |
| | South | 2.24 | 2.34 | 1.41 | 1.49 |
| Spring Average | North | 1.71 | 1.97 | 0.74 | 0.95 |
| | Central | 2.77 | 2.85 | 1.12 | 1.30 |
| | South | 2.41 | 2.43 | 1.37 | 1.55 |
| Summer Average | North | 1.95 | 2.21 | 1.35 | 1.85 |
| | Central | 3.17 | 3.49 | 2.04 | 2.14 |
| | South | 3.70 | 3.94 | 2.23 | 2.33 |
| Fall Average | North | 1.03 | 1.12 | 0.72 | 0.98 |
| | Central | 1.37 | 1.55 | 1.11 | 1.33 |
| | South | 1.95 | 2.09 | 1.25 | 1.48 |
| Winter Average | North | 0.75 | 0.85 | 0.45 | 0.45 |
| | Central | 1.08 | 1.15 | 0.70 | 0.64 |
| | South | 0.91 | 0.91 | 0.77 | 0.80 |

Table 0.2 Comparison of Atmospheric Heating Rates in Wm^{-2} in California calculated using independent modeling studies. The observationally constrained heating rates have an uncertainty of about ±60% compared with the 40% uncertainty in the TOA forcing.

VII.VIII. Regional climate impact results

To determine the climate impacts of BC, we performed two simulations, each covering 5 years for the 2005 - 2009 meteorological conditions. In one simulation, we used 2xBC to represent the conditions of the 2000s, and in the other simulation, we used 10xBC to represent the conditions of the 1960s (with BC reduced by a factor of five to approximate the historical COH records). Following this decreasing trend, we expect the top of the atmosphere (TOA) to cool.

1. *Overall, comparing the 2000s to the 1960s we find that the TOA radiative forcing decreases by up to $3 W m^{-2}$ (Figure 4) with larger and statistically*

significant changes at 90% confidence level in the summer and fall and over the Central Valley and southern CA.

The diabatic heating in the atmosphere is reduced by up to 0.06 K/day, and maximizes in the summer and at about 2 km above the surface. Reduction in BC leads to brightening at the surface as expected.

2. Corresponding to the enhanced surface solar radiation, skin temperature increases while the TOA radiative cooling leads to a cooling of atmospheric temperatures, but the average temperature changes are small (<0.1 C) and are not statistically significant due to the large interannual variability.

Winds at 10m generally become weaker over CA but stronger off shore in southern CA. Finally, changes in surface hydrology are small because the BC effects are generally small during winter, and BC is mostly concentrated in the Central Valley and southern CA, so its effects are negligible in the Sierra Nevada, which is where hydrology is most critical.

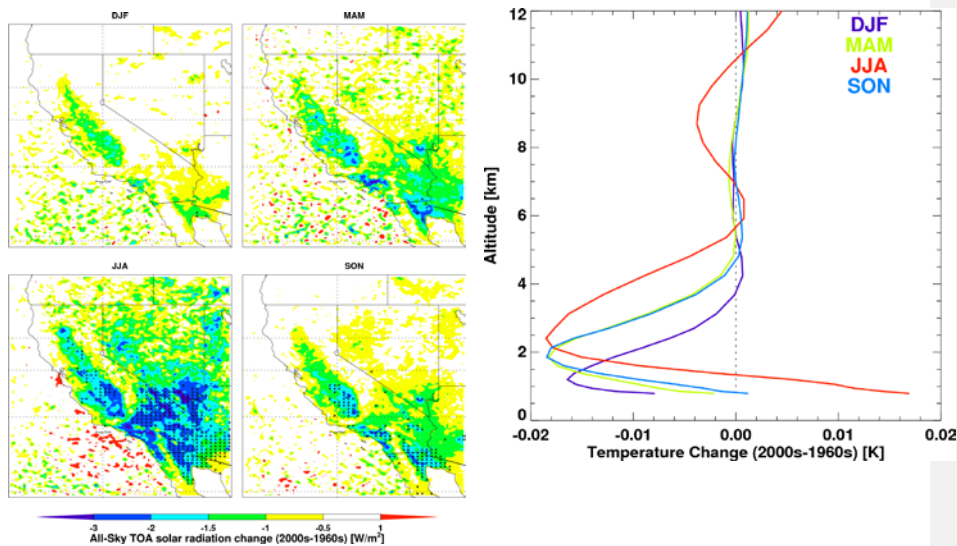


Figure 0.3 Changes in TOA solar radiation in the last 40 years attributed to BC decrease. Changes that are statistically significant at the 90% confidence level are stippled. The simulated atmospheric cooling and surface warming (only in summer) are shown on the right panel (not significant at the 90% level).

- 3. It appears that reduction of BC from the 1960s to 2000s produces a cooling of the lower atmosphere, accompanied by a statistically insignificant surface temperature changes.*

However, the larger scale and remote influence due to BC reduction over CA cannot be assessed in the regional modeling framework, which could also potentially affect the regional results over CA. In addition, the WRF-Chem model does not account for solar absorption by brown carbon. These uncertainties should be addressed in future studies.

Recommended future work

A more comprehensive understanding of the climate impacts of California's BC (+OC) mitigation on global and regional climate (including impacts on California's snow packs) processes requires further work along the following lines:

I. Global climate mitigation

- 1. We need to estimate the magnitude and uncertainty associated with the regional indirect and semi-direct effects through the OC_TD approach to better constrain the models.*

While the scope of this work was limited to determining the impact of BC, we discovered that BrC is also a significant absorber of radiation, particularly at short wavelengths and may serve as an extra warming agent due to its typically higher concentrations. The BrC is particularly important for California since our data reveals that open biomass burning is a large source for BrC. This opens up a whole new avenue of research as unlike BC, the sources, chemistry, and optical properties of BrC are less well understood. In particular we need to understand the following physic-chemical-optical properties of BrC:

2. What is the relative role of primary aerosols from biomass burning and diesel sources to BrC?
3. What is the relative role of secondary organics from biomass burning and diesel sources to BrC?
4. What are the intrinsic properties of BrC such as: size distribution, the single scattering albedo, and the angstrom exponent of absorption coefficient and scattering coefficient of BrC?
5. How does BrC within cloud drops and as interstitial aerosols in clouds enhance radiative forcing?

We recommend extensive future work, including field studies, laboratory studies, and data assimilation and modeling studies to better understand BrC. Further, current climate models do not consider BrC absorption and treat OC as a cooling

agent – while there still exists an uncertainty in the final sign of the net OC forcing we assert that climate models are overestimating its cooling impact.

In this report we presented several mitigation scenarios for BC that represent current and historical records of BC concentrations in California that are shown to be consistent with the control of diesel emissions. The mitigation scenarios considered in this study were constructed based on trends in California's aerosol concentrations. Although regional emissions are most important considering the short lifetime of BC, we did not consider variations in long-range transport (such as from Asia) in this study. Future studies should attempt to distinguish between transported and locally emitted BC.

II. Regional climate change

1. Continuation of EC/BC monitoring networks. The major findings of this study were made possible by the excellent networks of surface BC and column averaged aerosol optical properties. Unlike the long-lived greenhouse gases, documenting the impacts of mitigating short lived climate warmers such as BC requires continuation of such local and regional networks.

In the course of this study, we also discovered large uncertainties in existing data sets and resources that are currently used by climate scientists, such as in the solar flux measurements (Chapter 9) and the BC emission inventory (Chapter 11).

2. We recommend a more complete analysis of these resources and possible studies to implement better quality control, and to reduce the associated uncertainty.

3. Reducing uncertainty in regional model forcing: As documented here the OC_TD and EI_BU estimates of the forcing differ by a factor of almost two. Model treatment of EC and BrC emission inventory, optical effects, long range transport of BC from outside California, and vertical profiles of BC in models and simulation of clouds have to be validated first to bring the two approaches closer.

For example, an earlier study by us [Hadley et al., 2007] revealed that about 75% of BC above 2 km over California during spring time is transported from Eastern Asia.

4. A more detailed assessment of regional affects: The current study does not allow for the interaction with the larger scale circulation. Imbedding the WRF_Chem in a global model is required to simulate the potential changes in large-scale circulation due to BC reductions in CA.

5. The model does not account for solar absorption of OC, so the climate influence may be underestimated. In addition, it has been shown in an earlier study [Hadley and Kirchstetter, 2012] that snowfall deposits about 90% of the BC emissions to the snow packs of California, contributing to their melting.

6. Lastly, model biases and uncertainties in the model formulations and parameterizations, particularly related to clouds and aerosol-cloud interactions, should be addressed in the future to provide more robust simulations of BC climate effects.

